Inorg. Chem. **2005**, *44*, 1037−1043

Syntheses and Characterization of Oxo-Centered Triruthenium Compounds with Orthometalated Bipyridine

Jing-Lin Chen,[†] Xu-Dong Zhang,[†] Li-Yi Zhang,[†] Lin-Xi Shi,[†] and Zhong-Ning Chen*[,†,‡]

State Key Laboratory of Structural Chemistry, Fujian Institute of Research on the Structure of Matter and the Graduate School of CAS, The Chinese Academy of Sciences, Fuzhou, Fujian 350002, China, and State Key Laboratory of Organometallic Chemistry, Shanghai Institute of Organic Chemistry, The Chinese Academy of Sciences, Shanghai 200032, China

Received September 20, 2004

Reaction of oxo-centered triruthenium precursor compound $[Ru_3O(OAc)_6(py)_2(CH_3OH)](PF_6)$ (**1**) with 1.3 equiv of bipyridine ligand at ambient temperature gave oxo-centered triruthenium derivatives $[Ru_3O(OAc)_5\{\mu\text{-}\eta^1(C),\eta^2(N,N)\text{-bipyridine}\}(py)_2](PF_6)$ (bipyridine = 4,4′-dibutyl-2,2′-bipyridine (dbbpy) (**2**), 4,4′-dimethyl-2,2′-bipyridine (dmbpy) (**3**), 2,2′-bipyridine (bpy) (**4**), 5,5′-dibromo-2,2′-bipyridine (Br_2bpy) (**5**), 1,10-phenanthroline (phen) (**6**)). Formation of compounds **2**–**6** involved substitution of the axial methanol and one of bridging acetates in the precursor compound **1** by an orthometalated bipyridine. Reduction of **2** and **4** by addition of excess hydrazine gave one-electron-reduced neutral products $Ru_3O(OAc)_5(py)_2\{\mu\text{-}\eta^1(C),\eta^2(N,N)\text{-bipyridine}\}$ (bipyridine = dbbpy (**2a**), bpy (**4a**)). As established in the structure of **3** by X-ray crystallography, the orthometalated 2,2′-bipyridine adopts a $\mu\text{-}\eta^1(C),\eta^2(N,N)$ bonding mode. In the ^{1}H NMR spectra of **2**–**6**, the protons of acetate, pyridine, and bipyridine show obvious paramagnetic shifts. Tentative assignments of these proton signals were carried out. Absorption spectra of the bipyridine triruthenium derivatives show characteristic intracluster charge transfer (IC) transitions in the visible to near-infrared region (600–1000 nm) and cluster-to-ligand charge transfer (CLCT) transitions at 320–450 nm. By comparison of the redox data for **2**–**6**, it is concluded that introducing electron-donating substituents to the bipyridine favors stabilizing the $[Ru^{III}_3]^+$ and $[Ru^{III}_2Ru^{II}]^0$ states against disproportionation.

Introduction

It has been demonstrated that oxo-centered triruthenium−acetate cluster complexes with general formula $[Ru_3(\mu_3\text{-}O)(\mu\text{-}OAc)_6L_3]^+$ (L = axial ligands) show multiple redox behavior, intriguing mixed-valence chemistry, and versatile catalytic properties.[1−8] The axial ligands L are comparatively labile and can readily be substituted, thus enhancing significantly the richness of triruthenium chemistry. Axial ligand substitution affords an excellent means to control the chemical and electronic properties by introducing proper organic ligands. It also provides an approach to use the triruthenium clusters as potential building blocks for aggregated cluster complexes with higher nuclearity and desired

* Author to whom correspondence should be addressed. E-mail: czn@ms.fjirsm.ac.cn. Fax: +86-591-8379-2346.
† Fujian Institute of Research on the Structure of Matter.
‡ Shanghai Institute of Organic Chemistry.

(1) (a) Spencer, A.; Wilkinson, G. *J. Chem. Soc., Dalton Trans*. **1972**, 1570−1577. (b) Spencer, A.; Wilkinson, G. *J. Chem. Soc., Dalton Trans*. **1974**, 786−792.
(2) Cotton, F. A.; Norman, J. G., Jr. *Inorg. Chim. Acta* **1972**, *6*, 411−419.
(3) Baumann, J. A.; Salmon, D. J.; Wilson, S. T.; Meyer, T. J.; Hatfield, W. E. *Inorg. Chem*. **1978**, *17*, 3342−3350.
(4) (a) Baumann, J. A.; Salmon, D. J.; Wilson, S. T.; Meyer, T. J. *Inorg. Chem*. **1979**, *18*, 2472−2479. (b) Baumann, J. A.; Wilson, S. T.; Salmon, D. J.; Hood, P. L.; Meyer, T. J. *J. Am. Chem. Soc*. **1979**, *101*, 2916−2920. (c) Wilson, S. T.; Bondurant, R. F.; Meyer, T. J.; Salmon, D. J. *J. Am. Chem. Soc*. **1975**, *97*, 2285−2287.
(5) (a) Abe, M.; Sasaki, Y.; Yamada, Y.; Tsukahara, K.; Yano, S.; Yamaguchi, T.; Tominage, M.; Taniguchi, I.; Ito, T. *Inorg. Chem* **1996**, *35*, 6724−6734. (b) Abe, M.; Sasaki, Y.; Yamada, Y.; Tsukahara, K.; Yano, S.; Ito, T. *Inorg. Chem*. **1995**, *34*, 4490−4498. (c) Abe, M.; Sato, A.; Inomata, T.; Kondo, T.; Uosaki, K.; Sasaki, Y. *J. Chem. Soc., Dalton Trans*. **2000**, 2693−2702. (d) Sasaki, Y.; Tokiwa, A.; Ito, T. *J. Am. Chem. Soc*. **1987**, *109*, 6341−6347.
(6) Kido, H.; Nagino, H.; Ito, T. *Chem. Lett*. **1996**, 745−746.
(7) Ye, S.; Zhou, W.; Abe, M.; Nishida, T.; Cui, L.; Uosaki, K.; Osawa, M.; Sasaki, Y. *J. Am. Chem. Soc*. **2004**, *126*, 7434−7435.
(8) (a) Toma, H. E.; Araki, K.; Alexiou, A. D. P.; Nikoloau, S.; Dovidauskas, S. *Coord. Chem. Rev*. **2001**, *219*−*221*, 187−234. (b) Dovidauskas, S.; Toma, H. E.; Araki, K.; Sacco, H. C.; Iamamoto, Y. *Inorg. Chim. Acta* **2000**, *305*, 206−213. (c) Toma, H. E.; Alexiou, A. D. P.; Dovidauskas, S. *Eur. J. Inorg. Chem*. **2002**, 3010−3017. (d) Nikolaou, S.; Toma, H. E. *Polyhedron* **2001**, *20*, 253−259.

10.1021/ic048681c CCC: $30.25
Published on Web 01/19/2005

properties. Solvent-coordinated triruthenium compounds such as $[Ru_3(\mu_3\text{-}O)(\mu\text{-}OAc)_6L_2(CH_3OH)]^+$,[3] $Ru_3(\mu_3\text{-}O)(\mu\text{-}OAc)_6(CO)L(H_2O)$,[6] and $Ru_3(\mu_3\text{-}O)(\mu\text{-}OAc)_6(CO)(CH_3OH)_2$[4] are the most useful precursors for designing ligand-linked oligomers of $Ru_3(\mu_3\text{-}O)(\mu\text{-}OAc)_6$ cluster. Dimers, trimers, and hexamers of triruthenium clusters linked by pyrazine, 4,4′-bipyridine, and diphosphine have been described which exhibit extensive electronic communications between the triruthenium units.[4,9−13]

In contrast with the lability of axial ligand L, bridging acetates of the oxo-centered triruthenium core $Ru_3(\mu_3\text{-}O)(\mu\text{-}OAc)_6$ are well stabilized by the six-membered bonding ring of the $Ru_2(O)(\mu\text{-}OAc)$ moiety. Although substitution of the bridging acetates by an organic ligand is likely attained under rigorous conditions, the oxo-centered triruthenium cluster core is usually damaged in the reactions. Attempting to displace the bridging acetates by some N-heterocyclic ligands under mild conditions, we carried out reaction of $[Ru_3(\mu_3\text{-}O)(\mu\text{-}O_2CR)_6L_2(CH_3OH)]^-$ with bipyridine ligand at ambient temperature. As expected, substitution of one of the acetates in the $Ru_3(\mu_3\text{-}O)(\mu\text{-}OAc)_6$ core by a deprotonated bipyridine indeed occurs to yield a derivative triruthenium core $Ru_3(\mu_3\text{-}O)(OAc)_5\{\mu\text{-}\eta^1(C),\eta^2(N,N)\text{-bipyridine}\}$. We describe herein the preparation and structural and spectroscopic characterization of oxo-centered triruthenium cluster derivatives $[Ru_3O(OAc)_5\{\mu\text{-}\eta^1(C),\eta^2(N,N)\text{-bipyridine}\}(py)_2](PF_6)$ containing an orthometalated bipyridine.

Experimental Section

Materials and Reagents. All operations were performed under dry argon atmosphere by using Schlenk techniques and vacuum-line systems. Solvents were dried by standard methods and distilled prior to use. The regents 4,4′-dibutyl-2,2′-bipyridine (dbbpy), 4,4′-dimethyl-2,2′-bipyridine (dmbpy), 2,2′-bipyridine (bpy), and 1,10-phenanthroline (phen) were commercially available from Acros. 5,5′-Dibromo-2,2′-bipyridine (Br_2bpy) was synthesized by the literature method.[14] The compounds $[Ru_3O(OAc)_6(py)_2(CH_3OH)](PF_6)$ (**1**), $[Ru_3O(OAc)_6(py)_3](PF_6)$ (**7**), and $Ru_3O(OAc)_6(py)_3$ (**7a**) were prepared by the procedures described in the literature.[3]

$[Ru_3O(OAc)_5\{\mu\text{-}\eta^1(C),\eta^2(N,N)\text{-dbbpy}\}(py)_2](PF_6)$ (2). A dichloromethane (25 mL) solution containing **1** (100.7 mg, 0.10 mmol) and 4,4′-dibutyl-2,2′-bipyridine (34.9 mg, 0.13 mmol) was stirred for 2 days at room temperature to give a green solution. It was then concentrated in vacuo, and the product was purified by alumina column chromatography using dichloromethane as an eluent. Yield: 53% (63 mg). Anal. Calcd for $C_{38}H_{48}F_6N_4O_{11}PRu_3$: C, 38.52; H, 4.08; N, 4.73. Found: C, 39.04; H, 4.04; N, 4.63. ES-MS [*m*/*z* (%)]: 1041 (100), $[M - PF_6]^+$; 994 (30), $[Ru_3O(OAc)_5(py)(dbbpy)(CH_3OH)]^+$. IR (KBr, cm^{-1}): ν 1614 (m, COO), 1545 (m, COO), 1417 (s, COO), 842 (s, PF_6).

$[Ru_3O(OAc)_5\{\mu\text{-}\eta^1(C),\eta^2(N,N)\text{-dmbpy}\}(py)_2](PF_6)$ (3). This compound was prepared by the same synthetic procedure as that of **2** using 4,4′-dimethyl-2,2′-bipyridine instead of 4,4′-dibutyl-2,2′-bipyridine. Yield: 56%. Anal. Calcd for $C_{32}H_{36}F_6N_4O_{11}PRu_3$: C, 34.91; H, 3.30; N, 5.09. Found: C, 34.73; H, 3.17; N, 5.07. ES-MS [*m*/*z* (%)]: 957 (100), $[M - PF_6]^+$; 849 (80), $[Ru_3O(OAc)_5(dmbpy)(CH_3OH)(H_2O)]^+$; 835 (55), $[Ru_3O(OAc)_5(dmbpy)(H_2O)_2]^+$. IR (KBr, cm^{-1}): ν 1607 (m, COO), 1551 (m, COO), 1417 (s, COO), 842 (s, PF_6).

$[Ru_3O(OAc)_5\{\mu\text{-}\eta^1(C),\eta^2(N,N)\text{-bpy}\}(py)_2](PF_6)$ (4). This compound was prepared by the same synthetic procedure as that of **2** using 2,2′-bipyridine instead of 4,4′-dibutyl-2,2′-bipyridine. Yield: 63%. Anal. Calcd for $C_{30}H_{32}F_6N_4O_{11}PRu_3$: C, 33.59; H, 3.01; N, 5.22. Found: C, 33.03; H, 3.01; N, 5.05. ES-MS [*m*/*z* (%)]: 929 (88), $[M - PF_6]^+$; 835 (45), $[Ru_3O(OAc)_5(bpy^-)(CH_3OH)_2]^+$; 821 (100), $[Ru_3O(OAc)_5(bpy)(H_2O)(CH_3OH)]^+$; 807 (67), $[Ru_3O(OAc)_5(bpy)(H_2O)_2]^+$. IR (KBr, cm^{-1}): ν 1607 (m, COO), 1550 (m, COO), 1402 (s, COO), 842 (s, PF_6).

$[Ru_3O(OAc)_5\{\mu\text{-}\eta^1(C),\eta^2(N,N)\text{-}Br_2\text{bpy}\}(py)_2](PF_6)$ (5). This compound was prepared by the same synthetic procedure as that of **2** using 5,5′-dibromo-2,2′-bipyridine instead of 4,4′-dibutyl-2,2′-bipyridine. Yield: 47%. Anal. Calcd for $C_{30}H_{30}F_6N_4O_{11}Br_2PRu_3$: C, 29.28; H, 2.46; N, 4.55. Found: C, 29.50; H, 2.80; N, 4.51. ES-MS [*m*/*z* (%)]: 1105 (62), $[(M - PF_6)(H_2O)]^+$; 1087 (100), $[M - PF_6]^+$. IR (KBr, cm^{-1}): ν 1608 (m, COO), 1544 (m, COO), 1424 (s, COO), 842 (s, PF_6).

$[Ru_3O(OAc)_5\{\mu\text{-}\eta^1(C),\eta^2(N,N)\text{-phen}\}(py)_2](PF_6)$ (6). This compound was prepared by the same synthetic procedure as that of **2** using 1,10-phenanthroline instead of 4,4′-dibutyl-2,2′-bipyridine. Yield: 71%. Anal. Calcd for $C_{32}H_{32}F_6N_4O_{11}PRu_3$: C, 35.04; H, 2.94; N, 5.11. Found: C, 35.49; H, 3.02; N, 4.92. ES-MS [*m*/*z* (%)]: 953 (100), $[M - PF_6]^+$. IR (KBr, cm^{-1}): ν 1608 (m, COO), 1543 (m, COO), 1403 (s, COO), 842 (s, PF_6).

$Ru_3O(OAc)_5(py)_2\{\mu\text{-}\eta^1(C),\eta^2(N,N)\text{-dbbpy}\}$ (2a). To a dichloromethane (25 mL) solution of **2** (118.5 mg, 0.100 mmol) was added dropwise an excess aqueous solution of hydrazine (ca. 50%) with stirring until the solution color became brown-yellow. A 25 mL volume of water was then added, and the mixture was stirred for 0.5 h. After the dichloromethane layer was separated by an extraction funnel, the solvent was removed at reduced pressure. The product was recrystallized by dichloromethane−hexane and dried in vacuo. Yield: 73%. Anal. Calcd for $C_{38}H_{48}N_4O_{11}Ru_3$: C, 43.89; H, 4.65; N, 5.39. Found: C, 43.86; H, 4.80; N, 5.03. IR (KBr, cm^{-1}): ν 1563 (m, COO), 1403 (s, COO).

$Ru_3O(OAc)_5(py)_2\{\mu\text{-}\eta^1(C),\eta^2(N,N)\text{-bpy}\}$ (4a). This compound was prepared by the same synthetic procedure as that of **2a** except that **4** was used in place of **2**. Yield: 69%. Anal. Calcd for $C_{30}H_{32}N_4O_{11}Ru_3$: C, 38.84; H, 3.48; N, 6.04. Found: C, 38.89; H, 3.76; N, 5.72. IR (KBr, cm^{-1}): ν 1560 (m, COO), 1409 (s, COO).

Crystal Structural Determination. Crystals of $3\cdot H_2O\cdot 1/2Et_2O$ suitable for X-ray diffraction were obtained by laying diethyl ether onto the dichloromethane/1,2-dichloroethane (v/v, 2:1) solution. A

(9) (a) Ito, T.; Hamaguchi, T.; Nagino, H.; Yamaguchi, T.; Kido, H.; Zavarine, I. S.; Richmond, T.; Washington, J.; Kubiak, C. P. *J. Am. Chem. Soc.* **1999**, *121*, 4625−4632. (b) Ito, T.; Hamaguchi, T.; Nagino, H.; Yamaguchi, T.; Washington, J.; Kubiak, C. P. *Science* **1997**, *277*, 660−663. (c) Ota, K.; Sasaki, H.; Matsui, T.; Hamaguchi, T.; Yamaguchi, T.; Ito, T.; Kido, H.; Kubiak, C. P. *Inorg. Chem.* **1999**, *38*, 4070−4078. (d) Yamaguchi, T.; Imai, N.; Ito, T.; Kubiak, C. P. *Bull. Chem. Soc. Jpn.* **2000**, *73*, 1205−1212. (f) Ito, T.; Imai, N.; Yamaguchi, T.; Hamaguchi, T.; Londergan, C. H.; Kubiak, C. P. *Angew. Chem., Int. Ed.* **2004**, *43*, 1376−1381.

(10) (a) Londergan, C. H.; Salsman, J. C.; Ronco, S.; Dolkas, L. M.; Kubiak, C. P. *J. Am. Chem. Soc.* **2002**, *124*, 6236−6237. (b) Londergan, C. H.; Salsman, J. C.; Ronco, S.; Kubiak, C. P. *Inorg. Chem.* **2003**, *42*, 926−928. (c) Zavarine, I. S.; Kubiak, C. P.; Yamaguchi, T.; Ota, K.; Matsui, T.; Ito, T. *Inorg. Chem.* **2000**, *39*, 2696−2698. (d) Londergan, C. H.; Kubiak, C. P. *Chem.—Eur. J.* **2003**, *9*, 5962−5969.

(11) Chen, J. L.; Zhang, L. Y.; Chen, Z. N.; Gao, L. B.; Abe, M.; Sasaki, Y. *Inorg. Chem.* **2004**, *43*, 1481−1490.

(12) Toma, S. H.; Nikolaou, S.; Tomazela, D. M.; Eberlin, M. N.; Toma, H. E. *Inorg. Chim. Acta* **2004**, *357*, 2253−2260.

(13) Abe, M.; Michi, T.; Sato, A.; Kondo, T.; Zhou, W.; Ye, S.; Uosaki, K.; Sasaki, Y. *Angew. Chem., Int. Ed.* **2003**, *42*, 2912−2915.

(14) Romero, F. M.; Ziessel, R. *Tetrahedron Lett.* **1995**, *36*, 6471−6474.

Table 1. Crystallographic Data for $3{\cdot}H_2O{\cdot}1/2Et_2O$

empirical formula	$C_{34}H_{42}F_6N_4O_{12.5}PRu_3$
temp, K	293(2)
space group	Pcca
a, Å	15.778(7)
b, Å	25.808(11)
c, Å	23.676(10)
V, Å^3	9641(7)
Z	8
ρ_{calcd}, g/cm^{-3}	1.591
μ, mm^{-1}	1.041
radiation (λ, Å)	0.710 73
unique reflcns	8443
obsd reflcns with $I > 2\sigma(I)$	7773
R1(F_o)[a]	0.0838
wR2(F_o)[b]	0.1957
GOF	1.212

[a] $R1 = \sum|F_o - F_c|/\sum F_o$. [b] $wR2 = \sum[w(F_o^2 - F_c^2)_2]/\sum[w(F_o^2)]^{1/2}$.

crystal coated with epoxy resin was measured on a Siemens SMART CCD diffractometer by the ω scan technique at the room temperature using graphite-monochromated Mo Kα ($\lambda = 0.710\ 73$ Å) radiation. An absorption correction by SADABS was applied to the intensity data. The structure was solved by direct methods, and the heavy atoms were located from the *E*-map. The remaining non-hydrogen atoms were determined from the successive difference Fourier syntheses. All the non-hydrogen atoms were refined anisotropically, whereas the hydrogen atoms were generated geometrically with isotropic thermal parameters. The structure was refined on F^2 by the full-matrix least-squares method using the SHELXTL-97 program package.[15] Crystallographic data for $3{\cdot}H_2O{\cdot}1/2Et_2O$ are summarized in Table 1. Full crystallographic data are provided in the Supporting Information.

Physical Measurements. Elemental analyses (C, H, N) were carried out on a Perkin-Elmer model 240C automatic instrument. Electrospray mass spectra (ES-MS) were recorded on a Finnigan LCQ mass spectrometer using dichloromethane−methanol as mobile phase. UV−vis absorption spectra in acetonitrile solutions were measured on a Perkin-Elmer Lambda 25 UV−vis spectrometer. Infrared spectra were recorded on a Magna750 FT-IR spectrophotometer with KBr pellets. ^{1}H NMR spectra were performed on a Varian UNITY-500 spectrometer in CD_3CN solutions with $SiMe_4$ as the internal reference. The cyclic voltammogram (CV) and differential pulse voltammogram (DPV) were made with a model 263A potentiostat/galvanostat in dichloromethane solutions containing 0.1 M $(Bu_4N)PF_6$ as supporting electrolyte. CV was performed at a scan rate of 100 mV s^{-1}. DPV was measured at a rate of 20 mV s^{-1} with a pulse height of 40 mV. Platinum and glassy graphite were used as counter and working electrodes, respectively, and the potentials were measured against an Ag/AgCl reference electrode. The potential measured was always referenced to the half-wave potentials of the ferrocenium/ferrocene ($E_{1/2} = 0$) couple.

Results and Discussion

As shown in Scheme 1, compounds **2**−**6** were prepared by reaction of the precursor compound $[Ru_3O(OAc)_6(py)_2(MeOH)](PF_6)$ (**1**) with 1.3 equiv of bipyridine at ambient temperature. A color change from blue to green arises from orthometalation of the bipyridine that is bound to the oxo-centered triruthenium cluster center. An attempt to directly prepare triruthenium derivatives **2**−**6** by reaction of the parent compound $[Ru_3O(OAc)_6(py)_3](PF_6)$ (**7**) with excess bipyridine, however, was unsuccessful. Thus, it appears that attaching a substitutable methanol site in the precursor compound **1** is crucial for formation of triruthenium derivatives **2**−**6**. As established by X-ray crystallography (vide infra), formation of triruthenium derivatives **2**−**6** was involved in substitution of the coordinating methanol as well as one of acetates in the precursor compound **1** by an orthometalated bipyridine in a μ-η^1(C),η^2(*N*,*N*) bonding fashion (Scheme 1). Reduction of the 1+ compounds **2** and **4** by addition of excess hydrazine afforded one-electron-reduced products $Ru_3O(OAc)_5\{\mu$-η^1(C),η^2(*N*,*N*)-bipyridine$\}$-$(py)_2$ (bipyridine = dbbpy (**2a**), bpy (**4a**)) with a color change from green to brown-yellow. The bipyridine triruthenium compounds were well-defined by elemental analyses, ES-MS spectrometry, and UV−vis, IR, and ^{1}H NMR spectroscopy and characterized by X-ray crystallography for **3**.

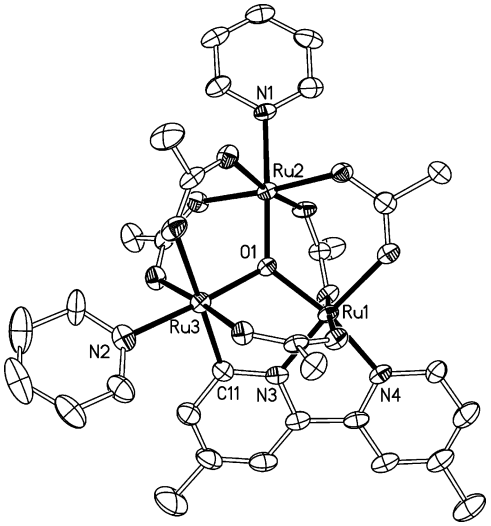

Figure 1. ORTEP drawing of the complex cation of **3** with atom-labeling scheme showing 30% thermal ellipsoids.

Scheme 1. Reaction of $[Ru_3O(OAc)_6(py)_2(CH_3OH)]^+$ with Bipyridine Ligand

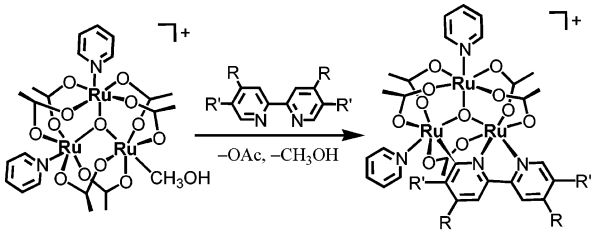

R = Bu^t, R' = H **2**; R = CH_3, R' = H **3**
R = H, R' = H **4**; R = H, R' = Br **5**

Selected atomic distances and bonding angles of **3** are presented in Table 2. A perspective view of the complex cation of **3** with atom numbering scheme is depicted in Figure 1. The complex $[Ru_3O(OAc)_5(dmbpy)(py)_2]^+$ can be viewed as a derivative of the parent complex $[Ru_3O(OAc)_6(py)_3]^+$ by substituting a deprotonated dmbpy for one of the bridging acetates and one pyridine. In a comparison of the interatomic distances of $[Ru_3O(OAc)_5(dmbpy)(py)_2]^+$ with those of its parent compounds $[Ru_3O(OOCR)_6(py)_3]^+$ and

(15) Sheldrick, G. M. *SHELXL-97, Program for the Refinement of Crystal Structures*; University of Göttingen: Göttingen, Germany, 1997.

Table 2. Selected Interatomic Distances (Å) and Bond Angles (deg) for **3**·H_2O·1/2Et_2O

Ru1···Ru2	3.361(6)	Ru1···Ru3	3.235(5)	Ru2···Ru3	3.369(6)
Ru1−O1	1.906(6)	Ru1−O2	2.060(7)	Ru1−O4	2.084(8)
Ru1−O6	2.049(7)	Ru1−N3	1.984(8)	Ru1−N4	2.063(8)
Ru2−O1	1.936(6)	Ru2−O3	2.032(7)	Ru2−O5	2.034(7)
Ru2−O8	2.038(7)	Ru2−O10	2.034(7)	Ru2−N1	2.104(8)
Ru3−O1	1.918(6)	Ru3−O7	2.053(7)	Ru3−O9	2.042(7)
Ru3−O11	2.171(8)	Ru3−C11	2.010(11)	Ru3−N2	2.117(10)
O1−Ru1−N3	89.4(3)	O1−Ru1−O6	92.8(3)	O1−Ru1−O2	92.8(3)
O1−Ru1−O4	95.4(3)	N3−Ru1−N4	78.8(4)	O6−Ru1−N4	91.7(3)
O2−Ru1−N4	83.0(3)	N4−Ru1−O4	96.5(3)	O1−Ru1−N4	167.3(3)
O1−Ru2−O3	93.8(3)	O1−Ru2−O5	94.0(3)	O1−Ru2−O10	96.4(3)
O1−Ru2−O8	92.2(3)	O3−Ru2−N1	85.9(3)	O5−Ru2−N1	87.8(3)
O10−Ru2−N1	84.0(3)	O8−Ru2−N1	85.9(3)	O1−Ru2−N1	178.1(3)
O1−Ru3−C11	89.8(3)	O1−Ru3−O9	94.5(3)	O1−Ru3−O7	90.6(3)
O1−Ru3−O11	92.7(3)	C11−Ru3−N2	95.1(4)	O9−Ru3−N2	87.2(3)
O7−Ru3−N2	87.7(3)	N2−Ru3−O11	82.4(4)	O1−Ru3−N2	174.8(3)
Ru1−O1−Ru2	122.0(3)	Ru1−O1−Ru3	115.6(3)	Ru2−O1−Ru3	121.9(3)

Table 3. ^{1}H NMR Chemical Shifts (δ) for Compounds **2**−**6**, **4a**, and **6a** in CD_3CN[a]

	2	**3**	**4**	**5**	**6**	**2a**	**4a**
δ(acetate)	16.245 (3H)	15.927 (3H)	15.256 (3H)	12.256 (3H)	15.956 (3H)	2.266 (3H)	2.420 (3H)
	7.591 (3H)	7.685 (3H)	7.782 (3H)	7.351 (3H)	7.086 (3H)	2.166 (3H)	2.171 (3H)
	4.761 (3H)	4.871 (3H)	4.921 (3H)	4.308 (3H)	4.279 (3H)	1.925 (3H)	2.101 (3H)
	−0.981 (3H)	−0.831 (3H)	−0.184 (3H)	−0.141 (3H)	−0.334 (3H)	1.893 (3H)	1.813 (3H)
	−2.200 (3H)	−1.993 (3H)	−1.536 (3H)	−1.068 (3H)	−1.487 (3H)	1.543 (3H)	1.646 (3H)
δ(bipyridine)	8.319 (1H, d)	8.065 (1H, d)	8.128 (1H, d)	8.239 (1H)	9.506 (1H)	9.344 (1H, g)	9.052 (1H, g)
	5.676 (1H, f)	5.736 (1H, f)	5.917 (1H, f)	5.991 (1H)	4.906 (1H)	8.391 (1H, a)	8.324 (1H, a)
	1.410 (9H, C_4H_9)	5.153 (3H, CH_3)	6.452 (1H, e)		6.592 (1H)	7.896 (1H, c)	8.184 (1H, c)
	−0.067 (9H, C_4H_9)	−0.758 (3H, CH_3)	4.323 (1H, b)		4.512 (1H)	1.584 (9H, C_4H_9)	7.814 (1H, b)
	−3.550 (1H, c)	−3.184 (1H, c)	−2.035 (1H, c)	−1.397 (1H)	−0.802 (1H)	7.260 (1H, d)	7.799 (1H, d)
	−11.313 (1H, g)	−10.890 (1H, g)	−10.062 (1H, g)	−5.289 (1H)	−4.400 (1H)	1.201 (9H, C_4H_9)	6.821 (1H, e)
	−21.552 (1H, a)	−20.388 (1H, a)	−20.241 (1H, a)	−13.225 (1H)	−13.829 (1H)	5.699 (1H, f)	6.485 (1H, f)
δ(py′)	9.233 (2H, α′)	9.291 (2H, α′)	9.322 (2H, α′)	7.258 (2H, α′)	8.975 (2H, α′)	9.408 (2H, α′)	9.229 (2H, α′)
	8.487 (1H, γ′)	8.400 (1H, γ′)	8.292 (1H, γ′)	7.987 (1H, γ′)	8.269 (1H, γ′)	8.176 (1H, γ′)	8.060 (1H, γ′)
	6.631 (2H, β′)	6.501 (2H, β′)	6.173 (2H, β′)	5.105 (2H, β′)	5.821 (2H, β′)	7.883 (2H, β′)	7.844 (2H, β′)
δ(py)	7.371 (1H, γ)	7.177 (1H, γ)	7.645 (1H, γ)	7.670 (1H, γ)	7.710 (1H, γ)	9.283 (2H, α)	9.052 (2H, α)
	5.773 (2H, β)	5.467 (2H, β)	4.627 (2H, β)	2.787 (2H, β)	3.717 (2H, β)	8.119 (1H, γ)	8.060 (1H, γ)
	1.299 (2H, α)	2.107 (2H, α)	2.168 (2H, α)	1.765 (2H, α)	1.822 (2H, α)	7.780 (2H, β)	7.844 (2H, β)

[a] ^{1}H NMR spectra (499.8 MHz) were recorded in CD_3CN at 298 K.

$[Ru_3O(OOCR)_6(py)_2L]^+$,[8a,9c,16,17] only slight differences are observed for the Ru···Ru and Ru−O_{oxo} distances. The Ru−$O_{acetate}$ (2.032(7)−2.084(8) Å) distances are also in the normal ranges except that one of them is much longer due to the remarkable trans effect caused by orthometalation of dmbpy, making the Ru3−O11 (2.171(8) Å) trans to the C donor elongated significantly relative to others. As shown in Figure 1, the orthometalated dmbpy exhibits a μ-η^1(C),η^2(*N*,*N*) coordination mode,[18−20] chelating the Ru1 center via its two N donors (N3 and N4) and bonding to the Ru3 center via the C11 donor adjacent to the N3 atom. The μ-η^1(C),η^2(*N*,*N*) bonding mode is favored by formation of two five-membered chelating rings as depicted in Figure 1. The Ru3−C11 (2.010(11) Å) distance is comparable to that observed in $Ru_2(CO)_5(C_{10}H_7N_2)(C_5H_4N)$ (2.11(1) Å)[18] and $[Ru_5(\mu\text{-H})C(CO)_3(C_{10}H_7N_2)]$ (2.053(9) Å, $C_{10}H_7N_2$ = deprotonated bipyridine).[19] The Ru−N distances (1.984(8) and 2.063(8) Å), however, are shorter obviously than those (2.04−2.23 Å) found in the ruthenium carbonyl compounds.[18,19] Relative to numerous complexes with metalated bipyridine described in the literature,[21] orthometalation of bipyridine in a μ-η^1(C),η^2(*N*,*N*) bonding mode only occurs in a few cases.[18−20] The three Ru^{III} centers are all located at distorted octahedral environments composed of O_4N_2, O_5N, and O_4NC chromophores for Ru1, Ru2, and Ru3, respectively. While the dihedral angle between Ru_3O and bipyridine planes is 36.5°, the Ru_3O plane forms dihedral angles of 13.0 and 18.8°, respectively, with two axially coordinated pyridine ligands.

The ^{1}H NMR spectral data for paramagnetic 1+ compounds **2**−**6** and one-electron-reduced diamagnetic products **2a** and **4a** are collected in Table 3 for the purpose of comparison. The spectrum of compound **2** showing its

(16) Abe, M.; Sasaki, Y.; Yamaguchi, T.; Ito, T. *Bull. Chem. Soc. Jpn*. **1992**, *65*, 1585−1590.
(17) Chen, J. L.; Yin, G. Q.; Chen, Z. N. *Chin. Chem. Lett.* **2003**, *14*, 519−522.
(18) Cockerton, B. R.; Deeming, A. *J. Organomet. Chem*. **1992**, *426*, C36−C39.
(19) Freeman, G.; Ingham, S. L.; Johnson, B. F. G.; McPartlin, M.; Scowen, I. J. *J. Chem. Soc., Dalton Trans*. **1997**, 2705−2711.
(20) Deeming, A. J.; Peters, R.; Hursthouse, M. B.; Backer-Dirks, J. D. J. *J. Chem. Soc., Dalton Trans*. **1982**, 787−791.
(21) See for example: (a) Minghetti, G.; Stoccoro, S.; Cinellu, M. A.; Soro, B.; Zucca, A. *Organometallics* **2003**, *22*, 4770−4777 and references herein. (b) Barigelletti, F.; Ventura, B.; Collin, J.-P.; Kayhanian, R.; Gaviña, P.; Sauvage, J.-P. *Eur. J. Inorg. Chem*. **2000**, *113*, 113−119. (c) Stoccoro, S.; Soro, B.; Minghetti, G.; Zucca, A.; Cinellu, M. A. *J. Organomet. Chem*. **2003**, *679*, 1−9. (d) Lai, S.-W.; Chan, M. C.-W.; Cheung, T.-C.; Peng, S.-M.; Che, C.-M. *Inorg. Chem*. **1999**, *38*, 4046−4055. (e) Mikel, C.; Potvin, P. G. *Inorg. Chim. Acta* **2001**, *325*, 1−8. (f) Constable, E. C.; Rees, D. G. F. *Polyhedron* **1998**, *17*, 3281−3289.

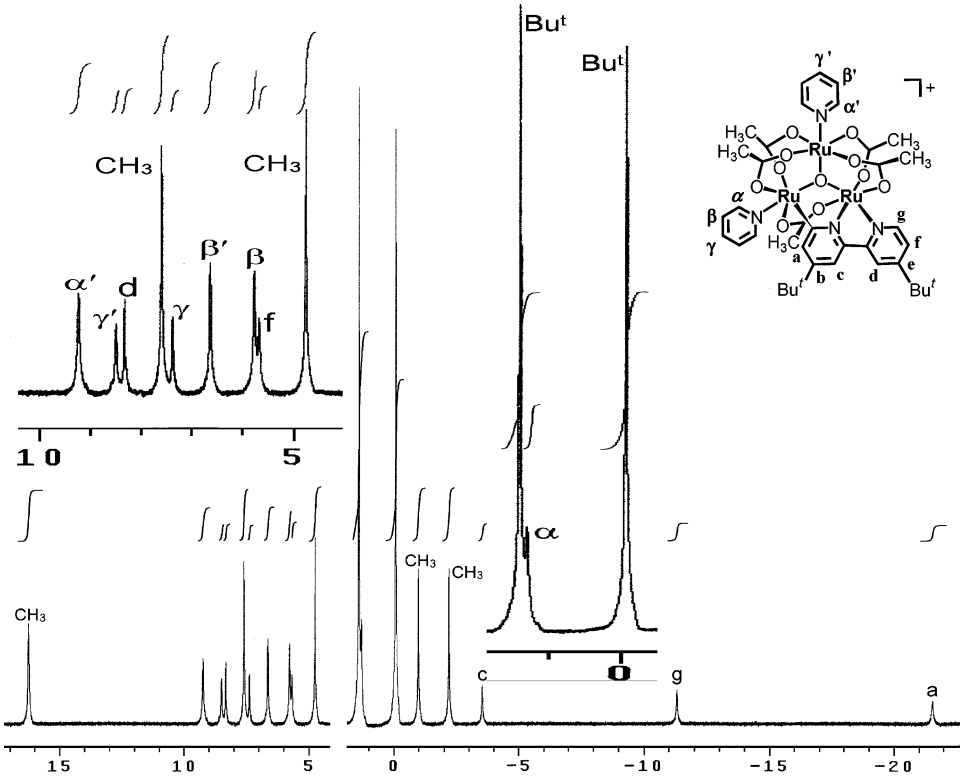

Figure 2. ^{1}H NMR spectrum of **2** in CD_3CN at 298 K.

characteristic proton signals is depicted in Figure 2. By reference to the assignment of orthometalated bipyridine in the ^{1}H NMR spectrum of diruthenium carbonyl compound $Ru_2(CO)_5(C_{10}H_7N_2)(C_5H_4N)$ ($C_{10}H_7N_2$ = deprotonated bipyridine),[18] the bipyridine proton signals in the diamagnetic neutral triruthenium derivatives **2a** and **4a** are tentatively assigned. In a comparison of the ^{1}H NMR spectra of **2a** and **4a** with those of the parent compound $Ru_3O(OAc)_6(py)_3$ (**7a**),[3,8a] the pyridine and acetate protons are also assigned unambiguously. As indicated in Table 3, five separate acetate CH_3 signals were observed at 2.42−1.54 ppm because of the low molecular symmetry caused by orthometalation of 4,4′-dibutyl-2,2′-bipyridine and 2,2′-bipyridine in **2a** and **4a**, respectively.

Relative to the corresponding proton signals in diamagnetic neutral complexes **2a** and **4a**, those in 1+ triruthenium compounds **2**−**6** show obvious paramagnetic shifts due to the influence of the unpaired electron in the latter. The line widths of the proton signals, however, are only broadened inappreciably. The proton number in each position or in each group can be recognized readily by comparison of the relative intensity of the signals as shown in the ^{1}H NMR spectrum of **2** (Figure 2). The acetate CH_3 protons in the 1+ paramagnetic triruthenium compounds **2**−**6** occur at 16.2 to −2.2 ppm. It is obvious that the acetate methyl protons in **2**−**6** show selective paramagnetic shifts, in contrast with the shifts to lower fields in the parent compounds $[Ru_3O(OAc)_6(L)_3]^+$ (L = axial ligand).[3,8a] Relative to the acetate CH_3 protons observed at 2.42−1.65 ppm in diamagnetic products **2a** and **4a**, of the five acetate CH_3 in **2**−**6**, three shift to lower fields whereas other two to higher fields. The opposite shifts for two different groups of acetate CH_3 is likely induced by orthometalation of the bipyridine, reflecting the different geometrical positions of the five acetates relative to the spatial character of the unpaired electron density.

For paramagnetic compounds **2**−**6**, the chemical shifts of various protons in the orthometalated bipyridine are tentatively identified by comparison of the variations induced by modification of the 4,4′- or 5,5′-substituents in 2,2′-bipyridine. It appears that the protons adjacent to the coordinating bipyridine N donors shift remarkably to higher fields, but those apart from the N donors show slightly paramagnetic shifts. Paramagnetic shifts of the orthometalated bipyridine protons may arise from pseudocontact through space magnetic interactions between the ligands and unpaired spin density localized within the Ru−O−Ru cluster framework.[3,8a] The weak cluster-to-bipyridine charge-transfer bands (vide infra) suggest that bipyridine π^* interactions with the metal orbitals in the 1+ triruthenium compounds of orthometalated bipyridines are not significant. Because of the low molecular symmetry, the two axially bonding pyridine ligands are spatially inequivalent so as to afford two set of separate proton peaks for the *ortho* (H_α and $H_{\alpha'}$), *meta* (H_β and $H_{\beta'}$), and *para* (H_γ and $H_{\gamma'}$) protons. As indicated in Figure 2 (compound **2**), the *ortho* and *meta* proton signals afford double intensity relative to the *para* ones. The *ortho* protons (H_α and $H_{\alpha'}$) are more sensitive to the local paramagnetic effects induced by the metal centers than the *meta* ones (H_β and $H_{\beta'}$). It is noteworthy that the paramagnetic shifts of the pyridine protons to higher fields in **2**−**6** are less pronounced than those in the parent cluster complexes $[Ru_3O(OAc)_6(py)_3]^+$ (**7**) and $[Ru_3O(OAc)_6(py)_2L']^+$.[3,8a] In

Table 4. Absorption Spectral Data for Compounds **2**−**7**, **4a**, **6a**, and **7a** in Acetonitrile

	λ_{max}/nm (ϵ/dm^3 mol^{-1} cm^{-1})		
	IC[a]	CLCT[b]	ligand−centered transitns
2	683 (6850)	425 (5100)	244 (30 740), 283 (29 090)
3	683 (7070)	430 (4700)	244 (31 100), 282 (29 470)
4	683 (6760)	434 (4600)	242 (30 880), 285 (27 280)
5	692 (5170)	445 (4070)	244 (25 030), 306 (23 330)
6	693 (6200)	384 (9560)	223 (41 280), 258 (38 090)
7	689 (5520)	320 (9190)	240 (21 610)
2a	806 (7570), 902 (7990)	368 (12 490)	249 (30 030), 290 (23 660)
4a	802 (6100), 898 (6070)	353 (10 780)	248 (25 360), 290 (19 180)
7a	908 (8950)	389 (11 460)	248 (24 380)

[a] IC is intracluster transition. [b] CLCT is cluster-to-ligand charge-transfer transition.

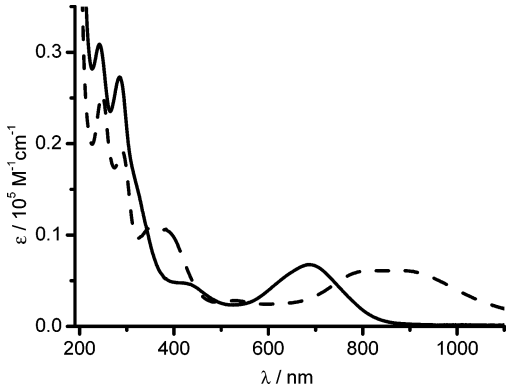

Figure 3. Electronic absorption spectra of compounds **4** (solid line) and one-electron-reduced product **4a** (dashed line) in acetonitrile.

fact, as aconsequence of the bipyridine orthometalation, while the protons in one pyridine are slightly shifted to higher fields, those in the other pyridine show almost no paramagnetic shifts.

The UV−vis spectral data of 1+ compounds **2**−**6** and their one-electron-reduced neutral products **2a** and **4a** in acetonitrile solutions at 298 K are summarized in Table 4. The electronic absorption spectra of **4** and its one-electron-reduced product **4a** are depicted in Figure 3. All of these compounds show characteristic absorption bands of the oxo-centered triruthenium clusters.[8a] It has been demonstrated that the low-energy bands in the visible to near-infrared region (600−1000 nm) are characteristic of an intracluster charge transfer (IC) transition in the oxo-centered triruthenium cluster compounds $[Ru_3(\mu_3\text{-}O)(\mu\text{-}OAc)_6L_3]^+$.[3,8a] In comparison with the low-energy bands of 1+ compounds **2**−**6**, those of one-electron-reduced neutral compounds **2a** and **4a** are remarkably red-shifted. The decrease in energy for these transitions by one-electron reduction reflects a rise of the occupied d_π levels as the number of electrons increases.[8a] The intermediate energy bands at 320−450 nm are highly sensitive to the oxidation states as well as the nature of the bipyridine ligand,[3,4] supporting an assignment of cluster-to-ligand charge transfer (CLCT) transition from the occupied d_π orbitals of triruthenium cluster to the lowest unoccupied π^* orbitals of the bipyridine ligand.[8a] Additionally, the acetates and N-heterocyclic ligands are responsible for the high-energy bands in the ultraviolet region, assigned to $\pi \rightarrow \pi^*$ transitions of the aromatic rings.

Table 5. Electrochemical Data for Compounds **2**−**7**[a]

	$E_{1/2}^{2+/+}$	$E_{1/2}^{+/0}$	$E_{1/2}^{0/-}$	$\Delta E'_{1/2}$[b]	$\Delta E''_{1/2}$[c]
2	+0.531	−0.623	−1.974	1.154	1.351
3	+0.516	−0.627	−1.977	1.143	1.350
4	+0.572	−0.569	−1.904	1.141	1.335
5	+0.613	−0.502	−1.811	1.115	1.309
6	+0.589	−0.537	−1.843	1.126	1.306
7	+0.592	−0.597	−1.986	1.189	1.389

[a] Potential data in volts vs F_c/F_c^+ ($E_{1/2} = 0$) are from single-scan cyclic voltammograms recorded at 25 °C. Detailed experimental conditions are given in the Experimental Section. [b] $\Delta E'_{1/2} = E_{1/2}^{2+/+} - E_{1/2}^{+/0}$. [c] $\Delta E''_{1/2} = E_{1/2}^{+/0} - E_{1/2}^{0/-}$.

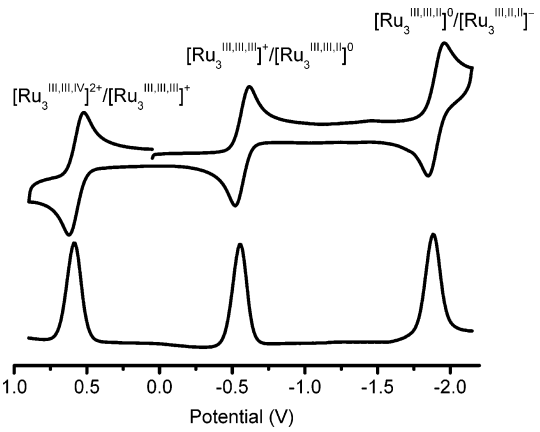

Figure 4. Cyclic and differential pulse voltammograms (CV and DPV) of compound **4** in 0.1 M dichloromethane solution of $(Bu_4N)PF_6$. The scan rates are 100 mV s^{-1} for CV and 20 mV s^{-1} for DPV.

The redox chemistry of compounds **2**−**6** has been investigated by cyclic and differential pulse voltammetry, and the data are presented in Table 5. The plots of cyclic and differential pulse voltammograms for compound **4** are shown in Figure 4. Three reversible redox waves in the range +1 to −2.0 V are observed in the cyclic and differential pulse voltammograms of compounds **2**−**6**, assigned to one-electron redox processes $[Ru^{IV}Ru^{III}_2]^{2+}/[Ru^{III}_3]^+$ ($E_{1/2}^{2+/+}$), $[Ru^{III}_3]^+/[Ru^{III}_2Ru^{II}]^0$ ($E_{1/2}^{2+/+}$), and $[Ru^{III}_2Ru^{II}]^0/[Ru^{III}Ru^{II}_2]^-$ ($E_{1/2}^{0/-}$), respectively.[3,8a] As shown in Table 5, all of the potentials $E_{1/2}^{2+/+}$, $E_{1/2}^{+/0}$, and $E_{1/2}^{0/-}$ are gradually positive-shifted with the increase of π-electron accepting ability in the bipyridine from compounds **2** to **5**. It is also interesting to note that both the potential gaps $\Delta E'_{1/2}$ ($\Delta E'_{1/2} = E_{1/2}^{2+/+} - E_{1/2}^{+/0}$) and $\Delta E''_{1/2}$ ($\Delta E'_{1/2} = E_{1/2}^{+/0} - E_{1/2}^{0/-}$) for the compounds are ordered **2** > **3** > **4** > **5**. Consequently, the stabilizations against disproportionation for the oxidation states $[Ru^{III}_3]^+$ and $[Ru^{III}_2Ru^{II}]^0$ are in the order **2** > **3** > **4** > **5**. Relative to the bipy compound **4**, introducing electron-donating substituents in compounds **2** and **3** favors stabilizing the $[Ru^{III}_3]^+$ and $[Ru^{III}_2Ru^{II}]^0$ states, whereas attaching electron-withdrawing substituents in compound **5** would destabilize it against disproportionation.[11] Moreover, in comparison with those ($\Delta E'_{1/2}$ = 1.189 V and $\Delta E''_{1/2}$ = 1.389 V) in the parent triruthenium complex $[Ru_3O(OAc)_6(py)_3]^+$ (**7**), both $\Delta E'_{1/2}$ (1.154−1.115 V) and $\Delta E''_{1/2}$ (1.351−1.306 V) in orthometalated bipyridine triruthenium derivatives **2**−**6** decrease, thus lowering stability of the $[Ru^{III}_3]^+$ and $[Ru^{III}_2Ru^{II}]^0$ states against disproportionation.

Conclusion

A synthetic route has been established to prepare oxo-centered triruthenium cluster derivatives of orthometalated bipyridine by reaction of oxo-centered triruthenium precursor compound $[Ru_3O(OAc)_6(py)_2(CH_3OH)](PF_6)$ with bipyridine at ambient temperature. Substitution of one of bridging acetates in the oxo-centered triruthenium cluster core $Ru_3O(OAc)_6$ by a orthometalated bipyridine affords a derivate triruthenium cluster core $Ru_3(\mu_3\text{-}O)(OAc)_5\{\mu\text{-}\eta^1(C),\eta^2(N,N)\text{-}$bipyridine$\}$. From structural and spectroscopic characterization, it has been demonstrated that substitution of one of bridging acetates by an orthometalated bipyridine affects slightly the electronic, chemical, and physical characteristics of the oxo-centered triruthenium cluster compounds. The synthetic strategy described herein would open a significant approach for the design of multifunctional materials with oxo-centered triruthenium cluster units containing bis- or tris-(bipyridine). Further study is being pursued.

Acknowledgment. This work was supported by the NSFC (Grants 20171044, 20273074, and 20490210), the NSF of Fujian Province (Geants E0420002 and E0310029), the fund from the Chinese Academy of Sciences, and the national basic research program (Grant 001CB108906) from the Ministry of Sciences and Technology of China.

Supporting Information Available: ES-MS and ^{1}H NMR spectra of compounds **2**−**6**, **2a**, and **4a** and X-ray crystallographic files in CIF format for the structure determination of compound **3**·H_2O·1/2Et_2O. This material is available free of charge via the Internet at http://pubs.acs.org.

IC048681C